

Roughening Instability and Evolution of the Ge(001) Surface during Ion Sputtering

E. Chason, T. M. Mayer, B. K. Kellerman, D. T. McIlroy, and A. J. Howard

Sandia National Laboratories, Albuquerque, New Mexico 87185

(Received 21 January 1994)

We have investigated the temperature-dependent roughening kinetics of Ge surfaces during low energy ion sputtering using energy dispersive x-ray reflectivity. At 150°C and below, the surface is amorphized by ion impact and roughens to a steady state small value. At 250°C the surface remains crystalline, roughens exponentially with time, and develops a pronounced ripple topography. At higher temperature this exponential roughening is slower, with an initial sublinear time dependence. A model that contains a balance between smoothing by surface diffusion and viscous flow and roughening by atom removal explains the kinetics. Ripple formation is a result of a curvature-dependent sputter yield.

PACS numbers: 61.80.Az, 61.80.Jh, 68.10.Et, 81.60.Cp

The evolution of surface morphology during deposition or sputtering of surfaces is the result of a balance between multiple roughening and smoothing processes. Stochastic addition or removal of material tends to roughen the surface while transport driven by surface energy minimization tends to smoothen the surface. Determining the dynamic response of the surface can provide important insight into the interaction of these various surface processes. Conversely, understanding the interaction among these various surface processes is essential to the atomic-level control of surface morphology.

Recent advances in scanning probe microscopies have greatly enhanced our understanding of roughness [1]. However, kinetic studies of the roughening process with this approach are very difficult. Although the various continuum theories of surface evolution predict scaling laws in both the spatial and temporal domains [2,3], most work thus far has concentrated on the development of spatial correlations.

There have been some recent reports of surface roughening kinetics measured by other techniques. Zuo and Wendelken [4] have used low energy electron diffraction to examine the evolution of Cu surfaces during growth; An *et al.* [5] have used spectroscopic ellipsometry to measure surface roughening as a consequence of cluster nucleation in amorphous Si film growth. X-ray reflectivity has also been shown to be a sensitive probe of surface roughness; several studies of roughening kinetics have been reported for synchrotron-based experiments [6,7]. Recently, we have developed an x-ray reflectivity technique that allows us to rapidly measure surface roughness with conventional x-ray sources [8,9].

In this work, we present kinetic measurements of ion-induced roughening and smoothing of Ge(001) surfaces over a range of temperatures from 150 to 350°C. We interpret the kinetics in terms of a linear model of the surface evolution which includes a curvature-dependent roughening term, and surface transport processes which smoothen the surface. The roughening process leads to a surface instability which favors the exponential growth of a selected range of spatial frequencies. We also show that surface transport processes depend on material struc-

ture. Surface diffusion is the primary smoothing mechanism on crystalline surfaces, while viscous flow is dominant for amorphous surfaces.

We perform the x-ray reflectivity measurements on a rotating-anode-based *in situ* energy dispersive reflectometer. Details of this technique have been published elsewhere [9]. Low energy ions are incident on the sample at an angle of 55° from normal, and along a $\langle 110 \rangle$ azimuth; the x rays are incident along a $\langle 100 \rangle$ azimuth. All experiments in this study use 1 keV Xe, with typical flux in the range 10^{12} – 10^{13} cm⁻²s⁻¹. A RHEED system (reflection high energy electron diffraction) in the sputtering chamber is used to determine the crystallinity of the substrate after ion bombardment.

Analysis of the reflectivity spectra is performed by fitting the experimental data to the reflectivity calculated from the Fresnel equations, including a Debye-Waller type factor to account for the surface roughness [10]. Assuming a Gaussian form of the surface electron density gradient we obtain a roughness parameter σ , the variance of the surface height profile. Typical measurements on as-prepared samples, before sputtering, give $\sigma \approx 0.1$ nm. The spectra were not corrected for off-specular background since measurements indicated this effect was not significant for the degree of roughness studied here. Measurements of in-plane structure are performed with a Digital Instruments Nanoscope III atomic force microscope (AFM).

The evolution of the roughness parameter at different substrate temperatures during Xe bombardment is shown in Fig. 1. In each case the flux is identical (2.5×10^{12} cm⁻²s⁻¹). Three distinct regimes of roughening are observed as a function of temperature. At the highest temperature shown (350°C), the surface is seen to roughen slowly with a time dependence that is sublinear. At lower temperature (250°C), the surface roughens exponentially with time. However, at still lower temperature (150°C), the surface roughness reaches a steady-state value that does not increase even after prolonged sputtering.

RHEED measurements after sputtering indicate that the surface remains crystalline during sputtering at 250°C and above, while at 150°C and below the surface

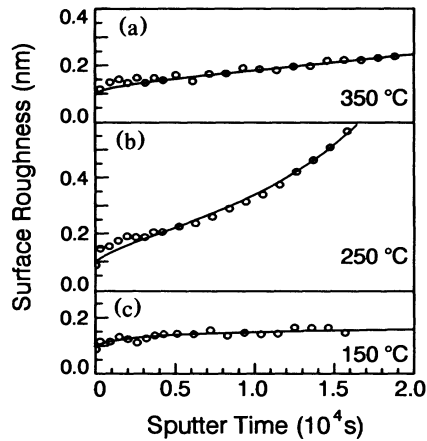


FIG. 1. Ge surface roughening kinetics at substrate temperatures of (a) 350°C, (b) 250°C, and (c) 150°C. The ion beam is 1 keV Xe with a flux of $3.2 \times 10^{12} \text{ cm}^{-2} \text{ s}^{-1}$. Solid lines are the results of model calculations based on Eq. (5).

becomes amorphous. This is consistent with previous studies of ion-induced amorphization [11]. To further investigate this sensitivity of the roughening kinetics to structure, we sputter the surface in the sequence shown in Fig. 2. Initially, the substrate is bombarded at 300°C. As in Fig. 1(b), the surface remains crystalline and roughens rapidly. The sputter-roughened sample is then allowed to cool and is bombarded again at room temperature. The surface amorphizes and the roughness decreases exponentially with time, clearly demonstrating differing roughening and smoothing kinetics depending on the crystalline nature of the surface.

To determine the in-plane structure of the ion-roughened surface, an AFM topograph was obtained from the Ge surface after irradiation at 300°C and a fluence of $1.0 \times 10^{17} \text{ cm}^{-2}$ and is shown in Fig. 3. Figure 3(a) shows a line scan taken along the direction of the ion beam on the surface [indicated by the solid line in Fig. 3(b)]. A surface periodicity with wave vector parallel to the ion beam direction is discernible, with wavelength on the order of 200 nm. The rms roughness as measured by the AFM over various $1 \mu\text{m}^2$ sections of the surface is $1.1 \pm 0.1 \text{ nm}$, in good agreement with the value of $1.2 \pm 0.05 \text{ nm}$ obtained from the x-ray measurement.

An adequate model of the surface morphology must account for the kinetics of roughening and smoothing of the surface, the temperature-dependent roughening rate, and the observation of a preferred orientation and period of the surface ripple structure. The evolution of an arbitrary surface can be understood most easily in terms of its spatial frequency spectrum,

$$h(\mathbf{q}, t) = \int g(\mathbf{r}, t) \exp(-i\mathbf{q} \cdot \mathbf{r}) d^2\mathbf{r},$$

where $g(\mathbf{r}, t)$ is the distribution of surface heights relative to the average, \mathbf{q} is the surface wave vector, and $h(\mathbf{q}, t)$ is the spectrum of spatial frequencies contained in the surface structure. The measured mean square roughness,

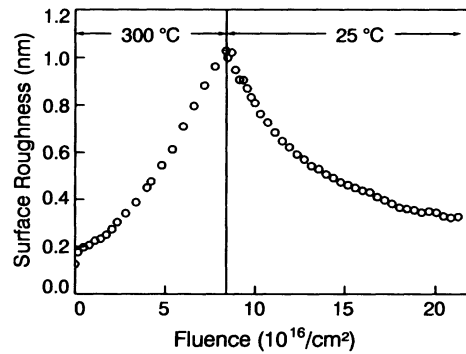


FIG. 2. Effect of surface crystallinity on roughening and smoothing kinetics. The sample is initially bombarded with 1 keV Xe at 300°C and a flux of $5.6 \times 10^{12} \text{ cm}^{-2} \text{ s}^{-1}$; surface remains crystalline during bombardment. After roughening at 300°C, the sample is cooled to room temperature and subsequently bombarded with the same energy ion beam at a flux of $3.7 \times 10^{12} \text{ cm}^{-2} \text{ s}^{-1}$; surface amorphizes during bombardment.

σ^2 , is related to the spatial frequency spectrum by

$$\sigma^2(t) = \int |h(\mathbf{q}, t)|^2 d^2\mathbf{q} / L^2, \quad (1)$$

where L is the lateral coherence length of the measurement. L is in the range 0.5–1.5 μm for the results discussed here.

The evolution of $h(\mathbf{q}, t)$ is determined by a number of roughening and smoothing processes. We consider the smoothing processes first. For the present work we limit these mechanisms to viscous flow and surface diffusion.

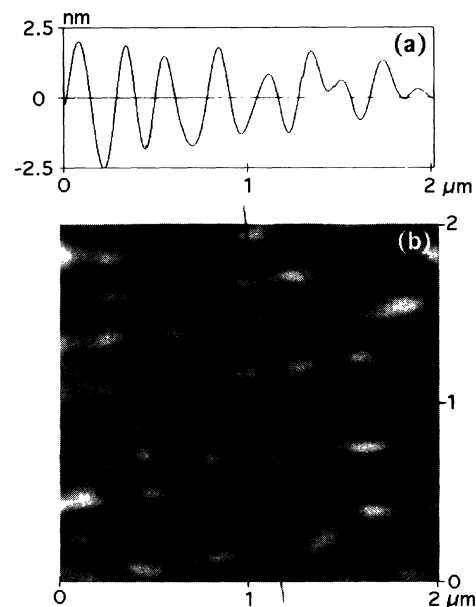


FIG. 3. (a) AFM line scan and (b) topograph of Ge surface after 1 keV Xe ion bombardment at 300°C. Sample was sputtered for 370 min with an incident flux of $4.8 \times 10^{12} \text{ cm}^{-2} \text{ s}^{-1}$. The solid line in (b) indicates the incident direction of the ion beam and the direction of the line scan in (a).

A periodic structure will decay according to [12,13]

$$d|h(\mathbf{q},t)|^2/dt = -(Fq + Dq^4)|h(\mathbf{q},t)|^2, \quad (2)$$

where $F = \gamma/\eta$ and $D = 2D_s\gamma\Omega^2\nu/kT$. Fq is the rate of relaxation by viscous flow and Dq^4 is the rate of relaxation by surface diffusion. η is the viscosity, D_s is the surface diffusivity, Ω is the atomic volume, and ν is the number of atoms per unit area of surface. The driving force for relaxation by both viscous flow and surface diffusion is reduction of the surface free energy, γ . The different dependence of these relaxation rates on the magnitude of the surface wave vector q shows that short wavelength surface features decay more rapidly by surface diffusion while viscous flow is more effective in the decay of long wavelength features.

Roughening of the surface is associated with material removal by sputtering. There is a stochastic roughening process, due to the random arrival of the ion at the surface. Assuming a Poisson-like process, this term, α , is expected to be independent of spatial frequency and amplitude (assuming no shadowing effects, which is appropriate for the amplitude of roughness discussed here). There is also a structure-dependent roughening term, first proposed by Bradley and Harper [14]. Using a calculation of sputter yield due to Sigmund [15], they recognized that the sputter yield depends on the surface curvature. This leads to a roughening term that is second order in q :

$$d|h(\mathbf{q},t)|^2/dt = Sq^2|h(\mathbf{q},t)|^2, \quad (3)$$

where

$$S = f[A_1 \cos^2(\varphi) + A_2 \sin^2(\varphi)]$$

and f is the ion flux, and φ is the azimuthal angle between the incident ion direction and the surface wave vector q . A_1 and A_2 are the curvature-dependent sputter yield coefficients, which depend on the range and lateral extent of energy deposition and on the angle of incidence. At the angle of incidence used in this work, we expect $A_1 > A_2 > 0$, so that surface features of all frequencies will grow exponentially, and are expected to have wave vectors in the same azimuthal direction as the ion beam.

The curvature-dependent effect results from the fact that the power deposition which causes sputtering is maximized below the surface. As a result, ions incident on a peak are likely to sputter atoms from the neighboring slopes, while ions incident on a trough are likely to sputter atoms near the trough. This model requires that the depth of energy deposition be much less than the radius of curvature of the structure. The estimated ion depth is approximately 2 nm, much less than the radius of curvature of 4×10^4 nm estimated from Fig. 3(a).

Combining these roughening and smoothing processes, we obtain the following linear equation governing the behavior of $h(\mathbf{q},t)$:

$$d|h(\mathbf{q},t)|^2/dt = R_q|h(\mathbf{q},t)|^2 + \alpha, \quad (4)$$

where

$$R_q = -Fq + Sq^2 - Dq^4.$$

Integrating this equation yields the time-dependent behavior of $h(\mathbf{q},t)$:

$$|h(\mathbf{q},t)|^2 = |h_0(\mathbf{q})|^2 \exp(R_q t) + (\alpha/R_q)[\exp(R_q t) - 1], \quad (5)$$

where $h_0(\mathbf{q})$ is the initial roughness spectrum.

From Eq. (5), we see that if R_q is positive the amplitude of that Fourier component will increase exponentially, while if R_q is negative, the amplitude will reach a steady-state value of $|\alpha/R_q|$. The maximum value of R_q determines the preferred wave vector q^* and the maximum rate of growth R^* ; the observed ripple pattern will have the wave vector q^* . Even if R^* is large, $|h(\mathbf{q},t)|^2$ initially grows linearly in time like a purely stochastic process if the starting surface is smooth; the amplitude at q^* must first be created by random fluctuations before it can be amplified by the instability.

Equation (5) explains the temperature dependence of the Ge roughening kinetics displayed in Fig. 1. At temperature $\geq 250^\circ\text{C}$ the surface remains crystalline, so the viscous flow mechanism of smoothing is inactive and $F=0$; in this case, we can solve explicitly to find $q^* [= (SD/2D)^{1/2}]$ and $R^* [= S^2/4D]$. Because the energy deposited in the sputtering process is much larger than thermal energies, we expect the value of S to be independent of temperature. At higher temperature, the value of D increases so that R^* decreases, and the surface roughens much more slowly. At temperatures lower than 150°C , however, the ion beam amorphizes the surface. Unlike crystalline surfaces, amorphous surfaces can relax by viscous flow as well as surface diffusion. Since F is no longer restricted to zero, R_q can be negative for all wave vectors, and $|h(\mathbf{q},t)|^2$ will reach a steady-state (small) value. This is apparent in the 150°C data of Fig. 1.

This model also predicts that in the absence of viscous relaxation, the maximum roughening rate ($R^* = S^2/4D$) depends on the square of the ion flux. We measured exponential roughening kinetics for fluxes of 1.4, 2.0, 2.5, and $3.1 \mu\text{A}/\text{cm}^2$ at a substrate temperature of 300°C and found that the exponential rate was in fact proportional to the square of the flux.

We obtain quantitative values of the coefficients S , F , and D by fitting this model to the observed kinetics. We calculate σ by numerically integrating Eq. (5) over q and φ . We obtain estimates of S and D at 300°C from the preferred periodicity (q^*) in the AFM topograph and the observed exponential roughening kinetics (R^*). The rate of smoothing in Fig. 2 is used to obtain an estimate of F at low temperatures. We have assumed S is anisotropic with azimuthal angle φ , such that $A_1/A_2=4$, which is consistent with the observed surface ripple orientation and with the predictions of Bradley's model, and the sto-

chastic roughening rate (α) is fit to the experimental data of Fig. 2.

The fits obtained from this model are shown as the solid lines in Fig. 1 with the following values used for the parameters: $S(\phi=0)=2\times 10^{-15}$ cm²/s; $S(\phi=90)=0.5\times 10^{-15}$ cm²/s; $F=1.0\times 10^{-9}$ cm/s for $T=150^\circ\text{C}$ and $F=0$ for $T\geq 250^\circ\text{C}$; $D=25, 7.2,$ and 0.8×10^{-27} cm⁴/s for $T=350, 250,$ and 150°C , respectively. The value of α is $2.4\times 10^{-20}/q_{\text{max}}^2$. Using a surface energy for Ge of 1.9 J/m^2 (see Ref. [16]), the surface diffusivity at 250°C obtained from D is 4.0×10^{-13} cm²/s, in reasonable agreement with values previously obtained from RHEED measurements of surface roughening [17]. The increase in surface diffusivity upon increasing temperature to 350°C corresponds to an activation energy of approximately 0.4 ± 0.1 eV. This is smaller than that estimated from the RHEED measurements, but consistent with the activation energy for surface self-diffusion of 0.65 eV estimated for Si(001) from scanning tunneling microscopy measurements [18].

Assuming the same values for γ and q^* as above, we obtain a value of the coefficient of viscosity of 1.6×10^{11} Ns/m². This is much lower than the thermally activated viscosity reported for relaxed amorphous Ge films [19], but within the range for radiation induced relaxation of bulk amorphous Si films [20]. This value is dependent on the ion flux, mass, and energy, and meaningful comparisons with bulk thermal relaxation behavior requires specification of defect density in both cases.

The value of $S(\phi=0)$, obtained from the measured roughening kinetics, is greater by a factor of 20 than that calculated using Bradley's formalism, and ion scattering parameters obtained from TRIM-90 [21]. One possible explanation lies in the fact that the Bradley theory assumes the surface is amorphous. Measurements of sputter yields on single crystal surfaces show a stronger dependence on surface orientation than amorphous surfaces [11] so the curvature dependence of the sputter yield for crystalline substrates may be greater than for amorphous materials. Indeed, measurements of roughening on amorphous SiO₂ surface do show better agreement with the calculated value of S [22].

The fact that this is a linear theory implies that each Fourier component evolves independently. Although we do not consider nonlinear terms, clearly at some amplitude these must become important due to processes such as shadowing. In the early stages reported here, the linear theory appears to be sufficient. At larger roughness values, we expect that the roughening kinetics should deviate from an exponential increase.

This work was supported by the U.S. Department of Energy under Contract No. DE-AC04-94AL85000. We thank Jerry Floro for useful discussions and insights.

-
- [1] E. A. Eklund, E. J. Snyder, and R. S. Williams, *Surf. Sci.* **285**, 157 (1993).
 - [2] F. Family and T. Vicsek, *J. Phys. A* **18**, L75 (1985).
 - [3] M. Kardar, G. Parisi, and Y. Zhang, *Phys. Rev. Lett.* **56**, 889 (1986).
 - [4] J. K. Zuo and J. F. Wendelken, *Phys. Rev. Lett.* **70**, 1662 (1993).
 - [5] I. An, Y. M. Li, C. R. Wronski, H. V. Nguyen, and R. W. Collins, *Appl. Phys. Lett.* **59**, 2543 (1991).
 - [6] A. A. Williams, J. M. C. Thornton, J. E. Macdonald, R. G. van Silfhout, J. F. Van der Veen, M. S. Finney, A. D. Johnson, and C. Norris, *Phys. Rev. B* **43**, 5001 (1991).
 - [7] H. You, R. P. Chiarello, H. K. Kim, and K. G. Vandervoort, *Phys. Rev. Lett.* **70**, 2900 (1993).
 - [8] E. Chason, T. M. Mayer, A. Payne, and D. Wu, *Appl. Phys. Lett.* **60**, 2353 (1992); E. Chason and T. M. Mayer, *Appl. Phys. Lett.* **62**, 363 (1993).
 - [9] E. Chason, T. M. Mayer, D. McIlroy, and C. M. Matzke, *Nucl. Instrum. Methods Phys. Res., Sect. B* **80/81**, 742 (1993).
 - [10] D. H. Bilderbeck, *SPIE Proc.* **315**, 315 (1981).
 - [11] H. E. Rosendahl, in *Sputtering by Particle Bombardment I*, edited by R. Behrisch (Springer, Berlin, 1981).
 - [12] C. Herring, *J. Appl. Phys.* **21**, 301 (1950).
 - [13] W. W. Mullins, *J. Appl. Phys.* **30**, 77 (1959).
 - [14] R. M. Bradley and J. M. E. Harper, *J. Vac. Sci. Technol. A* **6**, 2390 (1988).
 - [15] P. Sigmund, *Phys. Rev.* **184**, 383 (1970); *J. Mater. Sci.* **8**, 1545 (1973).
 - [16] J. M. Blakeley, *Introduction to the Properties of Crystal Surfaces* (Pergamon, Oxford, 1973); D. R. Clarke, in *The Mechanical Properties of Semiconductors*, edited by K. T. Faber and K. Malloy (Academic Press, Boston, 1992).
 - [17] E. Chason, J. Y. Tsao, K. M. Horn, S. T. Picraux, and H. A. Atwater, *J. Vac. Sci. Technol. A* **8**, 2507 (1990).
 - [18] Y. M. Mo, J. Kleiner, M. B. Webb, and M. G. Lagally, *Phys. Rev. Lett.* **66**, 1998 (1991).
 - [19] A. Witvrouw and F. Spaepen, *J. Appl. Phys.* (to be published).
 - [20] C. A. Volkert and A. Pohlman, *Mater. Res. Soc. Symp. Proc.* **235**, 3 (1992).
 - [21] J. F. Ziegler, J. P. Biersack, and U. Littmark, *The Stopping and Range of Ions in Solids* (Pergamon Press, New York, 1985).
 - [22] T. M. Mayer, E. Chason, and A. Howard (to be published).

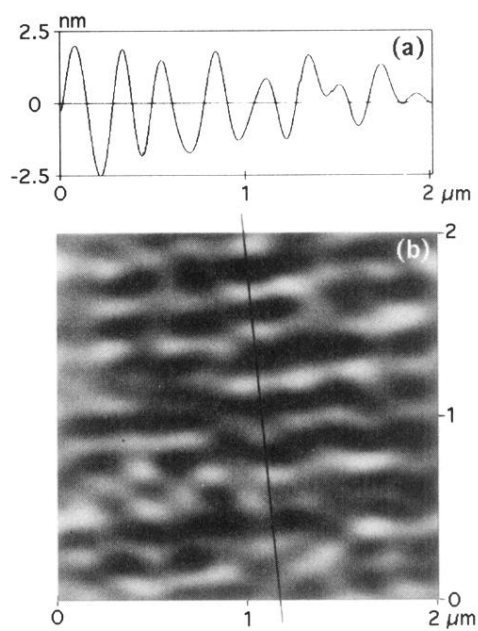


FIG. 3. (a) AFM line scan and (b) topograph of Ge surface after 1 keV Xe ion bombardment at 300°C. Sample was sputtered for 370 min with an incident flux of $4.8 \times 10^{12} \text{ cm}^{-2} \text{ s}^{-1}$. The solid line in (b) indicates the incident direction of the ion beam and the direction of the line scan in (a).